Evidence of an Unexpectedly Long C−C Bond (>2.7 Å) in 1,3-Metalladiyne Complexes $[Cp_2MCCR]_2$ (M = Ti, Zr): QTAIM and ELF Analyses

Isaac Vidal, Santiago Melchor, and José A. Dobado*

Grupo de Modelización y Diseño Molecular, Departamento de Química Orgánica, Universidad de Granada, Granada, Spain

Received: July 10, 2007; In Final Form: January 10, 2008

Topological analyses of the electron density using the quantum theory of atoms in molecules (QTAIM) and electron localization function (ELF) have been carried out, at the B3LYP/DGVZVP and MP2/DGVZVP theoretical levels, on different 1,3-metalladiyne cyclic compounds $[Cp_2M(CCR)]_2$, (M = Ti, Zr; R = F, CH_3, H, SiH_3). The QTAIM results indicate the presence of an extraordinarily long C−C bond (in a 2.7−3.0 Å range) connecting the CCR moieties, contrary to the common geometrical assumption of a M−M bond in similar metallacycles. The existence of this C−C bond is also supported by the distinct consequences on the reaction profiles for the Ti and Zr complexes, the CC oxidative coupling reactions being favored only for the Ti complexes. Moreover, the consequences of this bonding in the coupling/cleavage reactions of these metallacyclic complexes are reported and analyzed, revealing the transcendence of these long-range bonds in the overall behavior of these compounds.

Introduction

The discovery of several long C···C bonds in the range of 1.6−3.5 Å has been reported in organic molecules such as ortho-carboranes,[1] 3,8-dichlorocyclobuta[*b*]naphthalene derivatives,[2] and tetracyanoethylene anion dimers,[3] which constitute a challenge to the conventional bonding models. When compared to the length of any standard C−C bond, these bonds seem to have extraordinary length, which generally causes them to be disregarded as proper bonds. Their potential relevance as long-range mediators prompts their study to discover whether these bonds are strong enough to play a role in molecular reactivity.

Usually, in organometallic compounds, the presence of a metal atom results in a complete disruption of the normal behavior of organic molecules. This is the reason underlying their numerous applications in many chemical processes, such as in organic synthesis,[4] dehydrogenation reactions,[5] polymerization reactions,[6] and stereospecific reactions.[4] It is also known that metal atoms may induce weak interactions which, as the determination of the bond connectivity, sometimes are hard to determine.[7] For example, we have recently studied[8] the nature of the agostic bonds,[9,10] suggesting that some of the formerly considered α-agostic bonds are better viewed as agostic geometries, with no bonding to the metal, in which the hydrogen approximation is not caused by its bonding to the metal atom.

One of these reactions, in which weak interactions with metal atoms govern their geometrical structure, is the metal-catalyzed oxidative coupling of alkynes mediated by Ti atoms,[11] in which the 1,3-titanadiyne (see Scheme 1) plays a key role. These metallacyclic compounds, which were first isolated by Teuben,[12] participate also in other catalytic reactions applied to industrial processes,[13] acting as intermediates in the oxidative coupling reaction (see Scheme 2) of two phenylethynyl anions in the presence of two $[Cp_2Ti]$ groups and resulting in a strained but stable phenylbuta-1,4-diene product. Similar Zr-based complexes were prepared also by Erker,[14] but in contrast to Ti analogues, these do not yield the oxidative coupling reaction.[14,15]

SCHEME 1: General Molecular Arrangement of the Different 1,3-Metalladiyne Compounds Studied in This Work (1−8), Indicating the Specific Combination of R Groups and M Metal Atoms

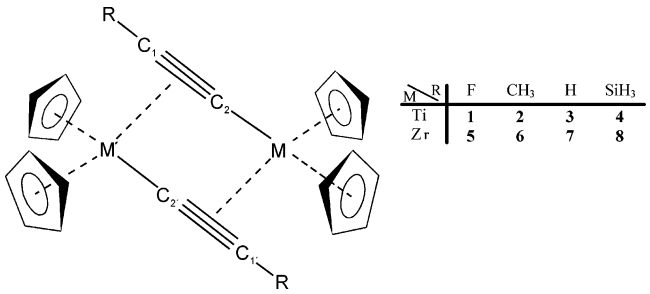

Bonding connectivity has constantly been an issue for these compounds because of the difficult determination of bonding interactions. Several models have been proposed to explain the interactions that yield such structures. Depending on the strength of each C···Ti interaction, these molecules can be viewed as dimers or proper metallacycles.[11] Despite having an ambiguous bonding structure, these compounds present notable stability. Moreover, another consequence of such labile bonds is a not fully understood reactivity.

The existence of a possible Ti···Ti bond was suggested by Stucky et al. to explain the observed diamagnetism.[11] The presence of a C···C bond was implicitly rejected, possibly to the large interatomic C···C distance (∼2.7 Å), presumed incompatible with bonding.[16] Nevertheless, in the 1980s, a pioneering study by Jemmis,[17] using the isolobal analogy from Extended Hückel and MNDO calculations, suggested the presence of a long-distance slight C···C interaction in Ti compounds, stating: "There is a slight bonding interaction that seems to develop." This, according to them does not lead to new C−C bond with Zr but does so with Ti. To the best of our

* Author to whom correspondence should be addressed. E-mail: dobado@ugr.es.

10.1021/jp075370p CCC: $40.75
Published on Web 03/15/2008

SCHEME 2: Schematic Structural Representation of the Geometries Adopted by the Reactive (a), TS (b), and Product (c) Molecules Calculated in the Present Work (1−8)

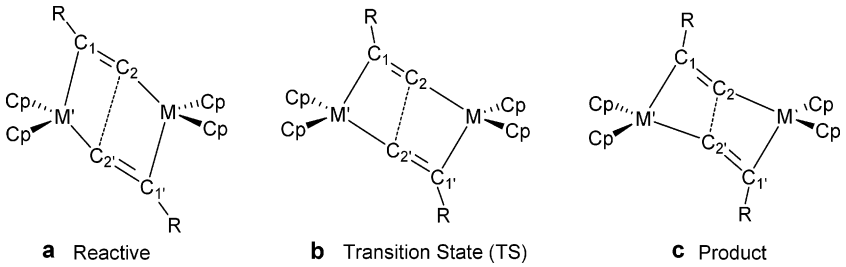

knowledge, no further studies supporting this idea, with links to the findings reported here, have been published.

Other comparative studies on these kinds of complexes were carried out by Rosenthal,[18] who analyzed in depth the coupling reactivity with Ti and Zr, oriented to synthetic applications in the metathesis reaction of 1,3-diynes. Nevertheless, the reasons why the Ti complexes are able to conduct the coupling reactions, while Zr does not, are still unknown.

However, the problem of distinguishing a bond within a complex molecular structure is not only associated with organometallic complexes but is ubiquitous in chemistry. As happens for other structures,[7,19] the existence of bonds is not always linked to the geometrical parameters (mainly short internuclear distances).

The bond concept, although being extremely useful for the chemist, is not an observable, in terms of quantum mechanics and therefore is subject to interpretation. Chemical models that include bonds as building blocks are usually forced to determine the existence or absence of bonds between atoms. Such theories are not always able to describe bonds properly, and therefore, determining the existence or absence of a bond could be somewhat arbitrary.

Geometric conditions are not the unique requirements for determine the presence of a bond, but electron arrangement has to be an integral part of the bond definition. Molecules are not a mere superposition of atoms, but atoms are glued together through bonds. The chemical ability of distinguishing an atom or functional group within a molecule implies that these retain their identity, so it is usually considered that bonds are entities that join atoms, these preserving part of their individual properties. At this point, given that molecular space can be divided into fragments (called open systems) in which the Schrödinger equation may be solved individually, it is reasonable to think that bonds are related to the boundary conditions between these open systems.

Based in these ideas, the theory that is able to identify the connectivity of bonds within molecules is the Quantum Theory of Atoms in Molecules (QTAIM), which has been also applied for characterization of long C−C bonds in tetracyanoethylene dimers[3] and ortho-carboranes.[1] The QTAIM, together with the analysis of the electron localization function (ELF) are useful tools for the identification of chemical structures (including bonding connectivity) and coupled electron pairs, respectively. Both approaches have been applied successfully to the characterization of other organometallic compounds.[8,20,21] Therefore, the main purpose of this work is to rationalize the bonding scheme for a set of different titana- and zirconadiyne complexes and uncover the causes of their distinct reactivity led by Ti and Zr atoms, within the framework of the QTAIM theory and ELF analysis. This has resulted in the identification of an uncommon C−C bond in 1,3-dimetallacycles, with bond lengths of about 2.7 Å. This finding corresponds to the above-mentioned prediction made by Jemmis.[17] Today, thanks to the availability of appropriate methodologies for the characterization of chemical bonding, we are able to uncover the presence of such bonds, which remained disregarded until now. Additionally, the consequences of this bonding in the reactivity of these metallacyclic complexes are reported and analyzed, revealing the transcendence of these long-range bonds in the overall behavior of these compounds.

Methodology

Calculations based on density functional theory (DFT) and MP2 were performed with the Gaussian03 package[22] for the determination of the geometries of the studied molecules, as well as for the further analysis of the resulting wavefunction. We used Becke's three-parameter functional[23] with the exchange potential of Lee, Yang, and Parr[24] (B3LYP), as in previous calculations on related organometallic compounds.[8] Nevertheless, the most relevant data of this work have been calculated also at the MP2 level (full core),[25] in order to validate the DFT results (see Table S-1). We chose the DGauss DZVP polarized DFT orbital basis sets for all atoms, coded in the Gaussian program as DGDZVP[26,27] which for Ti and Zr atoms acquires the (15s9p5d)/[5s3p2d] and (18s12p9d)/[6s5p3d] form, respectively. Although DGDZVP basis set lacks f functions for Ti and Zr, the validity of the geometric results arising from this basis set have been compared for compound **4a** against a more complete basis set including f and g functions, such as the Wachters−Hay function, which presents the form (15s11p6d3fg)/[10s7p4d3fg], employing the 6-311++G** basis set for the rest of the molecule. Results (see Table S-1) indicate no substantial geometric difference arising from the use of f and g functions. Also, the inclusion of the relativistic effects was considered in this work performing calculations on Zr complexes, using SBKJC[28] relativistic effective core potentials for Zr atoms and the DGDZVP basis set for the remaining atoms. Nevertheless, the geometries resulting from these calculations do no vary substantially, the $C_2-C_{2'}$ distances being even lower than those at B3LYP/ DGDZVP, and the energetic reaction profiles present almost no differences in comparison to the theoretical level chosen for this work (B3LYP/DGDZVP). For instance, Zr−C distances are systematically shorter with SBKJC in about 0.01 Å, while activation energies in the case of Zr compounds presenting the long C−C bond is 0.2 kcal·mol^{-1} higher with SBKJC, in the rest of the cases being 1 kcal·mol^{-1} lower. In any case, no substantial difference can be appreciated. A complete geometrical comparison of these two methods can be found in Tables S-3 and S-4 in the Supporting Information.

The stability[29,30] of the wavefunctions of all structures was checked through a relaxation of the wavefunction under various constraints: these comprise allowing an RHF determinant to become UHF or the orbitals to become complex. The results confirmed a singlet ground-state for all the structures. The local

stability of all structures was checked through the eigenvalues of the matrix of second derivatives (Hessian); all energetic minima presented no imaginary frequencies, while transition states (TS) presented a single imaginary frequency. Eventually the potential energy surface of these compounds were explored by performing a relaxed scan, in which the $C_2-C_{2'}$ distance was fixed and the rest of the geometrical parameters optimized.

The study of the bonding scheme present in these compounds was performed with the QTAIM[31−33] and ELF[34−37] methodologies. In QTAIM theory, the electron density topological analysis provides an accurate definition of the chemical concepts of atom, bond, and structure, as pointed out by Bader.[31−33] This theory allows the partition of the molecular space into separate regions associated with atoms, and thus an atom in a molecule is defined as the region of the space delimited by zero flux surfaces. For each point contained in the atomic basin, the gradient paths of the electron density lead to the atomic center with which the basin is associated. From the previous definition, the concept of bond between two atoms arises naturally: within a molecular system at equilibrium, two atoms are said to be bonded if they share a common interatomic surface (the zero-flux surface) through which they can interact, as is a common boundary condition for the independent resolution of the Schrödinger equation for each basin, this being the reason why atomic basins are also referred to as "*open systems*". This bonding condition is satisfied when there is a point (contained into the zero-flux surface) where the electron density is a minimum in a specific direction in space but a maximum in the plane perpendicular to it. These points are known as bond critical points (BCP), and the pair of gradient paths that connect the BCPs with each nucleus is referred to as the atomic interaction line or bond path.

With respect to the ELF function, this was first introduced by Becke and Edgecombe[34] and reinterpreted by Silvi and Savin[35] as a measure of the excess of local kinetic energy due to Pauli's exclusion principle, in comparison to a uniform electron gas. The ELF analyses, which is found elsewhere,[35−37] yield values are between 0 and 1. Values close to 1 indicate electron pairing at that point, whereas values near 0 are usually found in regions between electron pairs. As in QTAIM analysis, it is possible to divide the molecular domain in basins grouped around the ELF attractors. From a chemical standpoint, basins can be classified as being of core, valence, or hydrogenated. If the basin does not contain a nuclei, it is called a valence basin, whereas if it contains a nucleus other than a proton it is called a core basin, or hydrogenated if a proton is inside the basin. Valence basins are characterized by the number of core basins with which they are connected, and this is known as the synaptic order.[38] So, it provides valuable information about the location, size, population, and multiplicity of bonds, and most important, the degree of bond character reduction in those situations where the bond connectivity is not clear.

QTAIM data at the BCPs were calculated with MORPHY98,[39−41] while charges were integrated with AIM2000 Software.[42] ELF was computed with ToPMoD,[38] and isosurfaces were rendered with SciAn[43] visualization package.

Theoretical calculations were performed within these selected systems, and the geometry resulting from the optimization was compared to the closest structures for which X-ray data are available,[44,45] the formula differing only in the R substituent, $Si(CH_3)_3$. These structures (YATRAM, SAJCEL) were found in the Cambridge Structural Database (CSD).[46]

Results and Discussion

A. Geometrical and Energetic Features. As mentioned in the Introduction, a long C−C bond has been identified in some of 1,3-metalladiynes by the QTAIM analysis from B3LYP calculations. In addition, MP2 calculations were carried out for compound **4a**, in order to compare their results (See Table S-1 for geometric details and Figure S-14 for a representation of the C−C bond identified at the MP2 level). For the purpose of characterizing the origins and consequences of such bond, we have selected a set of model compounds with Ti and Zr modified with different substituents R = F, CH_3, H, and SiH_3. Two cyclopentadienyl (Cp) units were also attached to each metal atom as ligands, for a better modeling of the systems for which experimental data is available. Therefore, complexes can be viewed as the dimers of the organometallic compound $Cp_2M-C\equiv C$-R. The specific combination of metal atom M and substituent R are noted from **1** to **8**, corresponding **1**−**4** to Ti compounds and **5**−**8** to Zr ones, as indicated in Scheme 1.

In this work, we also seek to study the final step of the CC oxidative coupling reaction mechanism, and for that purpose, we characterized the molecular structures corresponding to reactives, TSs and products of this particular step. These are identified with Latin letters **a**−**c**, respectively. To verify the accuracy of the chosen methodological procedure, we compared calculated geometries with the experimental X-ray data in Figure 1. The X-ray data available correspond to similar Ti[45] and Zr[44] compounds, differing only in the R substituent, $Si(CH_3)_3$.

The structures of the CC oxidative coupling reaction analyzed here (**a**−**c**) present a similar geometry, both CCM moieties lying in the same plane. Additionally, the Cp rings are located above and below that plane, with their hydrogen atoms alternating as in a gear. For the reactives, resulting from the different interactions between C and M atoms, the structure of $[Cp_2M(CCR)]_2$ can be viewed as a dimer, where C_2 atoms are strongly attached to M, but C_1 atoms are attracted only to the M atom of the other monomer (see Figure 1). As the coupling reaction follows, the C_2 atoms are mutually attracted, finally resulting in a continuous butadiene-like structure (**c**) with two MCp_2 units joined to the carbon chain. All of these structures (**a**−**c**) can be considered also as metallacycles, because QTAIM identifies at least one ring in all of them.

In overall, the agreement of the calculated geometries with the experimental values can be qualified as good. In comparison with MP2 calculations performed with the same basis set (see Table S-1 for a methodological comparison for **4a**, B3LYP yields better geometries, closer to the experimental X-ray data. In general, differences between experimental and calculated data for **4a** and **8a** (molecules which best match the experimental molecules) are below 0.03 Å, except for M···M distances, where the differences rise to 0.08 Å. In general, MP2 results overestimate bond distances, up to 0.1 Å. Additionally, the M−M distance is shown to be very sensible to the specific substituent, lying in a range of 3.49−3.60 Å for Ti compounds, and 3.55−3.66 Å for Zr ones.

Figure 1 depicts the main geometrical features for the Ti and Zr reactive compounds (**2a**−**8a**). The F-substituted equivalent complex was not found for **1a**, but this issue is addressed below in the discussion of the reaction profiles. The most significant result arises from the comparison of the $M-C_2-M'-C_{2'}$ central moiety proportions, when comparing Ti and Zr complexes: proportions of the Ti-based compounds are notably wider than Zr-based ones, because, while the M···M distance remains almost similar (in an average of 3.56 Å for **1a**−**4a** and 3.60 Å for **5a**−**8a**), the $C_2\cdots C_{2'}$ distance for Zr compounds is 0.3 Å longer than in Ti ones. This results in a broadening of the central ring in the Ti structures. This trend is also observed in the X-ray

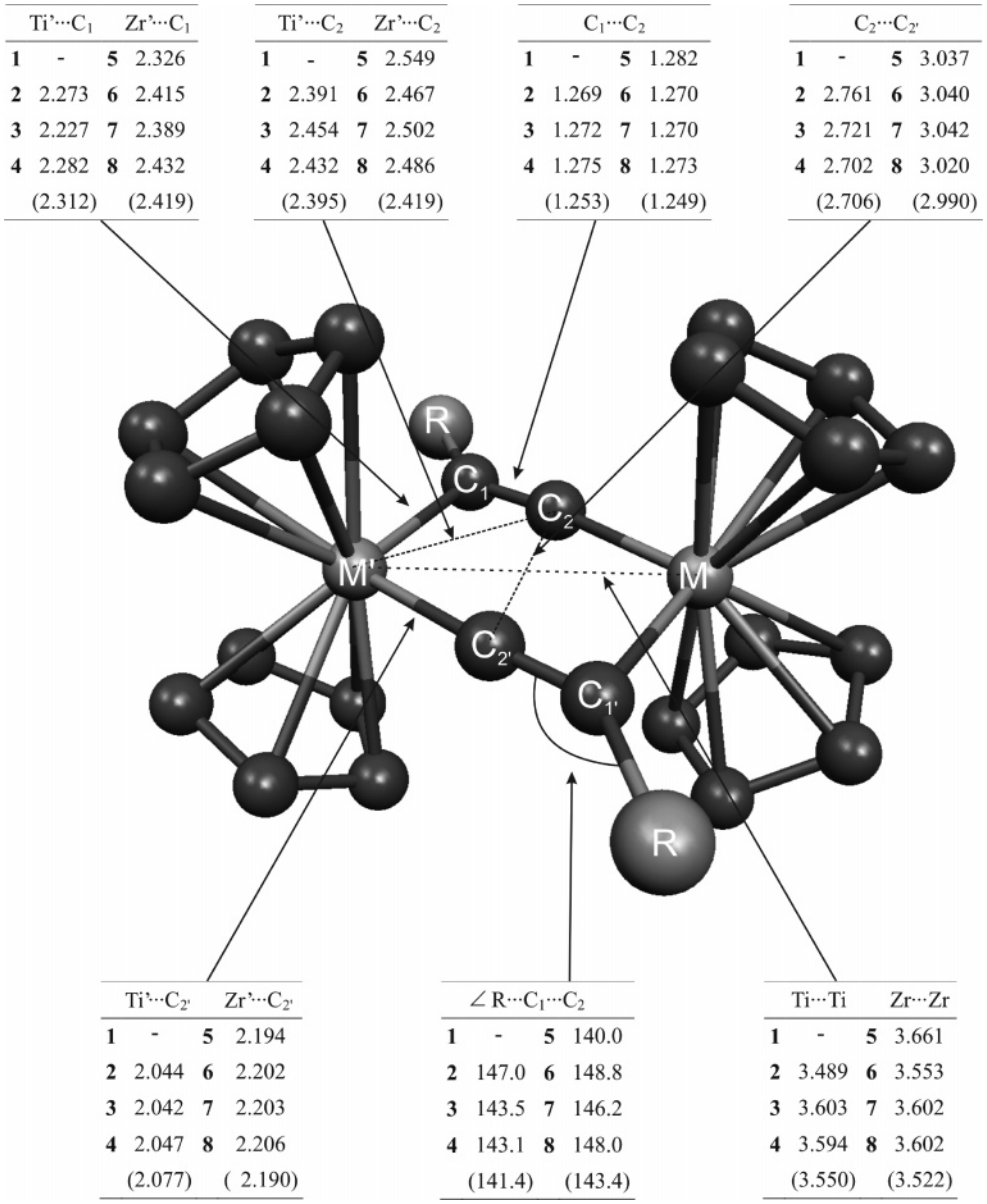

Figure 1. Geometrical parameters (angstroms and degrees) for **2a**−**8a** compounds calculated at the B3LYP/DGDZVP level. The experimental values appear in parentheses. All hydrogen atoms have been removed for clarity.

structures:[44,45] M···M distance is always of about 3.5 Å, but the C_2···$C_{2'}$ distance for Zr complexes is 0.3 Å greater.

Other geometric parameters that are increased from Ti to Zr are the M′−C_1 and M−$C_{2'}$ bond distances but to a lesser magnitude. Both of these are increased from Ti to Zr by about 0.16 Å, a value very similar to the covalent bond radius difference for Ti and Zr (0.13 Å). The C_1···C_2 distance remains almost unchanged with the different R substituent and metal atoms studied.

If the above-mentioned differences in the geometries were caused by the increase in atom size from Ti to Zr, this would be reflected in an overall resizing of the whole structure. Instead, only distances from the metal to the nearest atoms augmented and the M···M distance remains constant. This was noticed by Jemmis in 1988,[17] when it was associated with the possible existence of a M···M bond, which would be stronger for Zr than for Ti complexes. Nevertheless, although the strikingly C_2−$C_{2'}$ distance reduction from Zr to Ti was still noticed by Jemmis in 1998,[47] the question of whether the different distances indicate a C_2−$C_{2'}$ bond was left open.

The CC oxidative coupling reaction takes place following the compounds **a**−**c** indicated in Scheme 2. Simultaneous with the approaching of C_2 and $C_{2'}$ atoms the ∠RC_1C_2 angle is reduced to almost 130° for the transition states **1b**−**8b** (see Table S-4, in the Supporting Information). Other minor effects may also be appreciated: the C_1−C_2 bond is lengthened by about 0.03 Å for Ti compounds, and more than 0.04 Å for Zr complexes. Also, M′−C_1 is reduced from **a** to **b** compounds to a higher degree (about 0.14 Å and 0.18 Å for Ti and Zr compounds, respectively). This trend continues until the final stabilization of the products **c**: larger C_1−C_2 and shorter M′−C_1 bond distances, with an even lower valence angle (See Table S-5, in the Supporting Information). All of this evolution seems to be the result of a progressive destruction of the C_1≡C_2 triple bond, this being converted gradually into a double bond. As a consequence of these bond-order reductions, the bonds surrounding the C_1−C_2 bond are reinforced, and thus the incipient M'_1−C_1 bond is strengthened (shortened) and a new C_2−$C_{2'}$ is created.

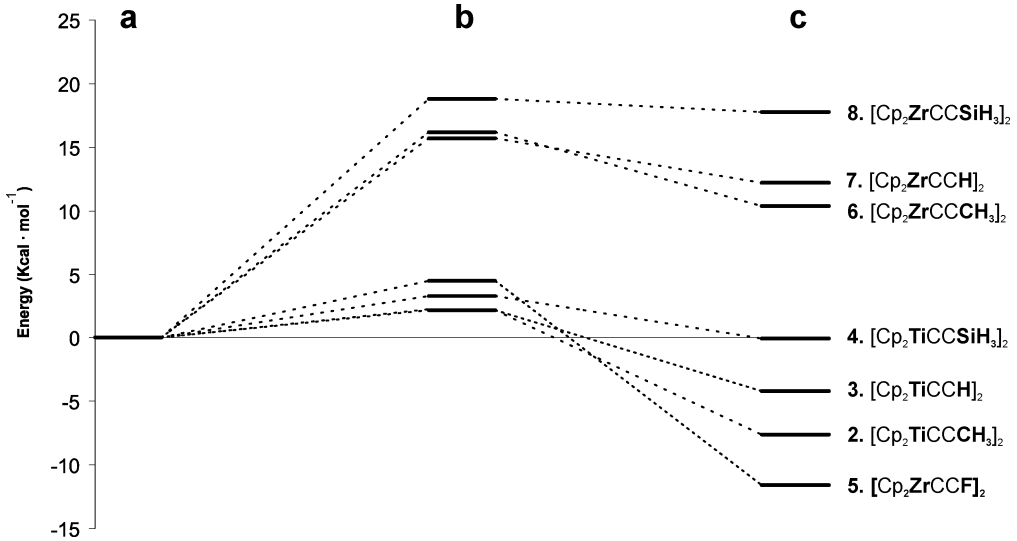

Figure 2. Relative energy profiles for **2**−**8** compounds in the last step of the CC oxidative coupling reaction of $[Cp_2MCCR]_2$ dimers, structures of TSs (b) and products (c). The reference origin is taken at the energy of the reactives (a). The values are corrected for the ZPVE.

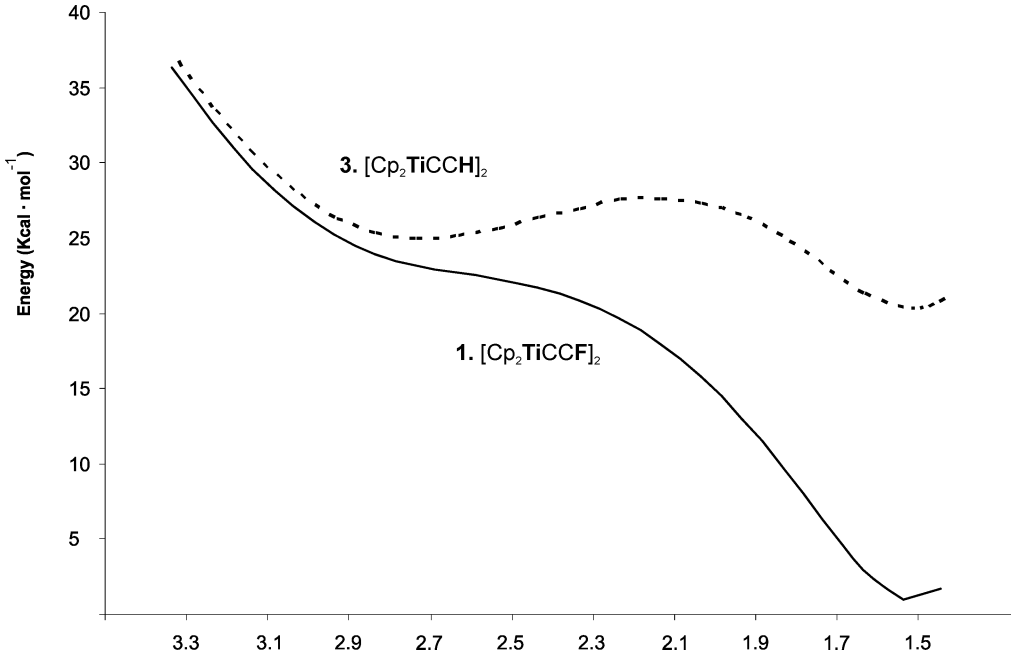

Figure 3. PES resulting from the variation of the $C_2\cdots C_{2'}$ distance in steps of 0.1 Å from 3.33 Å to 1.43 Å, for **1a** and **2a**. The *x*-axis is inverted for a better match with Figure 2.

Differences in the geometrical evolution of Ti and Zr compounds along the reaction path do not seem very evident, but the energetic profile of the reactions is appreciably different for all Ti and Zr compounds, as shown in Figure 2. For Ti complexes the reaction is exothermic, but by contrast, most Zr complexes yield to an endothermic reaction. Similarly, the reactions involving titanium yielded a low-energy barrier (about 3 kcal·mol^{-1}), while in most zirconium complexes these barriers were higher than 15 kcal·mol^{-1}, except for compound **5**, which presented an energy barrier of 5 kcal·mol^{-1}.

In order to determine the causes that avoided the finding of a reactive structure with fluorine within the Ti complexes (**1a**), an exploration of its potential energy surface (PES) has been carried out, and compared with that equivalent of structure **3a** with R = H (see Figure 3). In this picture, the energy of the system is calculated at fixed $C_2-C_{2'}$ distances, optimizing the remaining geometrical parameters. $C_2-C_{2'}$ distances for reactive structures (**a**) are about 2.9 Å, while distances for product structures (**c**) are near 1.5 Å. The main difference between PES for **1** and **3** is found in the number of minima present in the curve. While **3** resulted in two minima (**3a** and **3c**), the curve for **1** resulted in a single minimum (**1c**). The shape of the curve corresponding to **1** indicates that neither **1a** nor **1b** exists, but an indentation near 2.9 Å and the deep energetic bias show the effects caused by the presence of fluorine. In comparison to **3**, F has promoted the reaction in such manner that has lowered the energy barrier below the former value of the reactive, stabilizing the products, and a PES curve with a single minimum is observed.

From all the above results, the different reaction profiles seem to be caused by the presence of Ti or Zr in these complexes. The distance between C_2 and $C_{2'}$ depends strongly on the transition metal chosen, differing by a value much greater than the increase in atomic radius. Therefore, it might be asked whether the shorter $C_2\cdots C_{2'}$ distances for Ti complexes are related to the possible presence of a $C_2-C_{2'}$ bond. To answer this, we continue analyzing the arrangement of the electron distribution close to the center of the molecule.

B. Electronic Structure: QTAIM and ELF Analyses. The bond connectivity of these compounds is characterized within the QTAIM theory and the ELF analysis. If bonds were assigned using exclusively geometric criteria, as has been done implicitly in most of the literature,[16,18] this would result in both C_1 and C_2 bonded to M′, forming a three-membered ring, and possibly a bond connecting both metal atoms. Nevertheless, QTAIM shows clearly neither a bond path connecting M′ and C_2 nor a bond path connecting M and M′ for all the molecules studied. Instead, for certain compounds, an *a priori* unexpected $C_2-C_{2'}$ bond is found. This bond is more frequent for Ti compounds than for Zr compounds. More precisely, all the Ti compounds studied present a bond path connecting C_2 and $C_{2'}$, while within the Zr compounds, only **5a** shows such a bond. Additionally, the complementary calculations carried with MP2 over **4a** results also in the presence of a C2−C2′ bond path. (See Figure S-14). From Figure 2, it can be seen that the relative energies for the products are grouped in two, with a clear energy gap between them. All reactions for which reactive compounds present a $C_2-C_{2'}$ bond (including **5**) are considerably more favorable than those which do not. This indicates that the presence of such a long bond is related to the distinct reaction profiles. For the consequences and properties of this unusual bond to be clarified, a comprehensive bond characterization through the QTAIM and ELF analysis has to be performed.

Figure 4 shows a plot of the Laplacian of the electron density, $\nabla^2\rho(r)$, for Ti and Zr compounds **2a** and **6a** (R = CH_3) as representatives of compounds where this bond is present or absent, which includes the bond paths and critical points found. In this plot, a BCP appears in the geometric center of M, M′, C_2, and $C_{2'}$ atoms, connecting the two carbon atoms. The presence of a central BCP is also reflected in the appearance of two RCP at both sides of the $C_2-C_{2'}$ bond. For the other compounds (mostly Zr-based compounds, **6a**−**8a**), the BCP is replaced by a ring critical point (RCP) located at the same position. Although Zr seems to avoid the presence of such bond, an exception can be found in compound **5a**, where a clear BCP connects C_2 and $C_{2'}$ (see Table 1). This is due to the presence of the F atoms, as will be explained below.

These differences between Ti and Zr are added to the previously mentioned differing capability for yielding oxidative coupling reactions, properties which seem to be related to each other. Therefore, the possible link between these behaviors has to be addressed. It bears mentioning that the appearance of a BCP between C_2 and $C_{2'}$ atoms does not solely constitute an indication of the local shape of the electron density but also points out that both carbon atomic basins share a zero-flux surface, a boundary condition that is directly associated with the interaction between the electrons belonging to each basin.[31−33] The values of the electron density of this BCP may seem weak, but it has to be pointed out that, from the C_2 to the $C_{2'}$ atom, the atomic interaction line crosses zones close to both metal atoms. Therefore, compared to the high-density zones arising from the presence of the metals, the existence of a maximum of the electron density in the plane perpendicular to the $C_2-C_{2'}$ bond (the BCP), precisely between the M atoms, emphasizes the relative strength of this interaction.

The $C_2-C_{2'}$ interaction can be characterized by the properties of the corresponding BCP; the value of the electron density is always about 0.035 $e\cdot a_0^{-3}$, (see Table 1 and Figure 4). This is a relatively low value, but its order of magnitude is even higher than those found in other weak interactions, such as hydrogen bonding (about 0.014 $e\cdot a_0^{-3}$).[48] The Laplacian of the electron density, $\nabla^2\rho(r)$, is positive, indicating the presence of a charge-depletion zone associated with that BCP, as in most weak interactions. Despite the topological differences (different number of BCPs, RCPs, and bond paths) found between **2a** and **6a**, the remaining BCPs present similar values, but slight differences can be found in the C_2-M' bond, where ρ(r) is higher for compound **2a**.

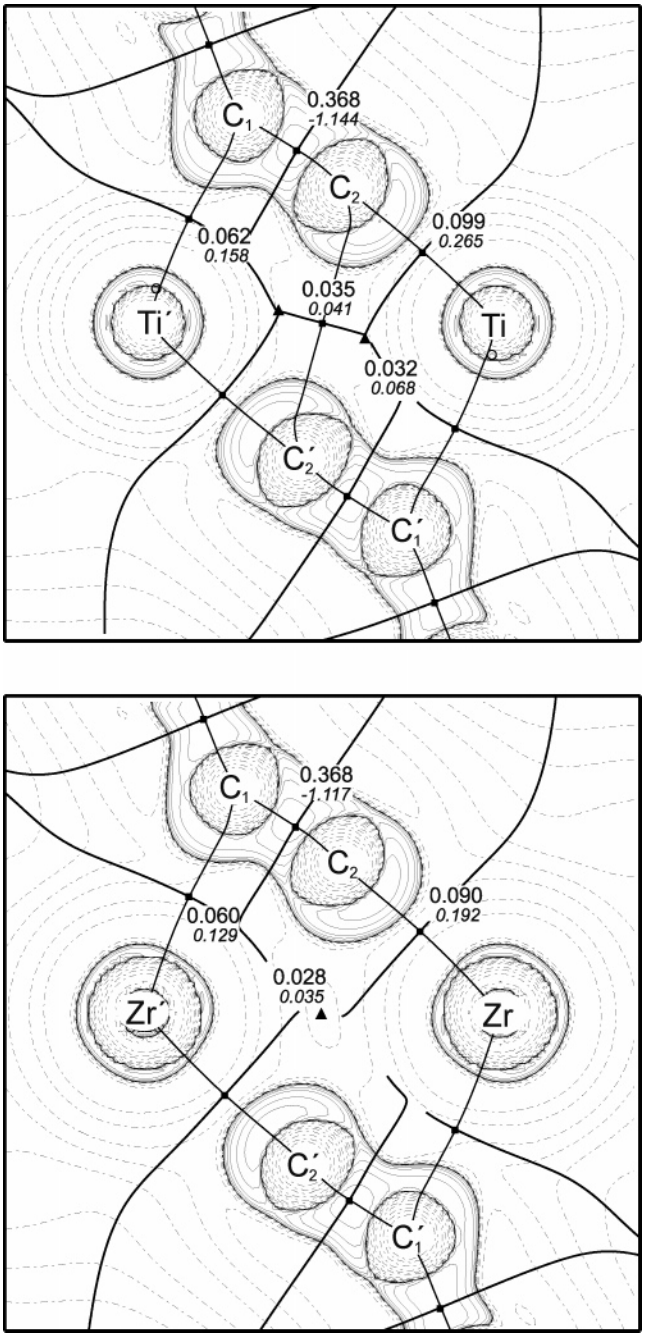

Figure 4. Laplacian plot of the electron density for **2a** (Ti) and **6a** (Zr), including the values of the electron density $\rho(r)$ ($e\cdot a_0^{-3}$), and, in italics, its Laplacian $\nabla^2\rho(r)$ ($e\cdot a_0^{-5}$) measured at the BCPs. The $\nabla^2\rho(r)$ contours begin at zero and increase (dashed contours) and decrease (solid contours) in steps of ±0.02, ±0.04, ±0.08, ±0.2, ±0.4, ±0.8, ±2.0, ±4.0, and ±8.0. The thick lines represent the atomic interaction lines joining the nuclei, solid squares represent the BCP, and solid triangles represent the RCP.

Table 1 lists the properties of the main bonds, including the $C_2-C_{2'}$ BCPs for **2a**−**8a**. Noticeably, **5a** (R = F) is the only Zr compound where a BCP joins the C_2 and $C_{2'}$ atoms. This raises the question as to whether the presence of a $C_2-C_{2'}$ bond

TABLE 1: Selected BCP Parameters for 1a−8a Calculated at the B3LYP/DZVP Level. Electron Density $\rho(r)$ ($e\cdot a_0^{-3}$), Its Laplacian, $\nabla^2\rho(r)$ ($e\cdot a_0^{-5}$), Electron Density Energy, $E_d(r)$(hartree$\cdot a_0^{-3}$), and Ellipticity, ϵ. The Values for Zr Compounds Are in Parentheses

		$\rho(r)$ ($e\cdot a_0^{-3}$)		$\nabla^2\rho(r)$ ($e\cdot a_0^{-5}$)		$E_d(r)$ (hartree$\cdot a_0^{-3}$)		ϵ	
$[Cp_2MCCR]_2$	R	Ti	Zr	Ti	Zr	Ti	Zr	Ti	Zr
				$C_2-C_{2'}$					
1a (5a)	F	–	(0.027)	–	(0.033)	–	(−0.01 1)	–	(6.581)
2a (6a)	CH_3	0.035	–	0.041	–	−0.019	–	1.246	–
3a (7a)	H	0.034	–	0.042	–	−0.018	–	1.185	–
4a (8a)	SiH_3	0.035	–	0.045	–	−0.019	–	1.247	–
				C_1-C_2					
1a (5a)	F	–	(0.358)	–	(−1.062)	–	(−0.679)	–	(0.277)
2a (6a)	CH_3	0.368	(0.368)	−1.144	(−1.117)	−0.689	(−0.701)	0.166	(0.130)
3a (7a)	H	0.367	(0.368)	−1.145	(−1.160)	−0.678	(−0.684)	0.156	(0.121)
4a (8a)	SiH_3	0.367	(0.369)	−1.108	(−1.161)	−0.698	(−0.682)	0.091	(0.061)
				C1−M′					
1a (5a)	F	–	(0.070)	–	(0.137)	–	(−0.068)	–	(0.173)
2a (6a)	CH_3	0.062	(0.060)	0.158	(0.129)	−0.052	(−0.055)	0.423	(0.612)
3a (7a)	H	0.067	(0.061)	0.160	(0.128)	−0.056	(−0.056)	0.236	(0.435)
4a (8a)	SiH_3	0.058	(0.055)	0.153	(0.131)	−0.048	(−0.051)	0.429	(0.806)
				C_2-M					
1a (5a)	F	–	(0.090)	–	(0.200)	–	(−0.101)	–	(0.212)
2a (6a)	CH_3	0.099	(0.090)	0.265	(0.192)	−0.105	(−0.099)	0.232	(0.268)
3a (7a)	H	0.099	(0.089)	0.273	(0.197)	−0.107	(−0.100)	0.231	(0.276)
4a (8a)	SiH_3	0.099	(0.089)	0.269	(0.194)	−0.106	(−0.099)	0.224	(0.262)

for **5a** is related to the absence of a Ti-based reactive structure **1a** (which would be equivalent to **5a**).

In both Ti and Zr complexes, the presence of fluorine causes the products to be much more stabilized. This can be seen for **1** in Figure 3, where although **1a** does not exist as a stable structure, one can extrapolate an estimate for the reaction energy from **1a** to **1c**. This value was estimated at about 25 kcal$\cdot$mol^{-1}, being exothermic.[49]

On comparing the increase of product stability from compounds with R = H and R = F, we find that, for Ti compounds (**3** and **1**), the additional stabilization caused by F is of about 22 kcal$\cdot$mol^{-1}, very similar to the stabilization of Zr compounds (**7** and **5**), where the energy of the products is lower by about 20 kcal mol^{-1}. The difference is that, while for Ti compounds the reactions preserves (but increases) its exothermic character, for Zr, the reaction changes its reaction behavior from endothermic to exothermic one.

It is remarkable that reactions with a bond path in the reactive structures gave an exothermic energetic profile. Therefore, it can be concluded that there is a direct correlation between the distinct reactivity and the presence of a bond, and we can affirm that the presence of this new type of C−C bond is the reason behind the formation of the butadiene hydrocarbon in this particular oxidative coupling reaction with Ti-based complexes. Moreover, the topology differences between **2a**−**5a** and **6a**−**8a** is related to the different energetic profiles described (lower reaction barriers for the former), because passing from the reactives to the products for **6a**−**8a** requires the formation of a catastrophe point (usually structures with higher instability) leading to higher reaction barriers before the formation of the new C−C bond. This condition was already achieved in **2a**−**5a**; the topology does not need to be changed from **a** to **c**, and therefore the activation barrier of the reaction is lower.

In the case of **1a**, the F atom does not solely produce the $C_2-C_{2'}$, but overwhelmingly stabilizes the product structure **1c**, causing the disappearance of the reaction barrier and also avoiding the existence of the TS **1b** and the reactive **1a**.

All $C_2-C_{2'}$ BCPs have properties similar to the BCP described above. Another parameter that shows remarkable values is ellipticity, with values up to 6.6 for compound **5a**.

TABLE 2: Integrated Electron Population over Selected QTAIM Atomic Basin of 1a−8a at the B3LYP/DGDZVP Level. See Scheme 1 for Atom Numbering.

		C_1	C_2	M
1a	$[Cp_2\mathbf{Ti}CC\mathbf{F}]_2$	–	–	–
2a	$[Cp_2\mathbf{Ti}CC\mathbf{CH_3}]_2$	6.54	6.41	20.26
3a	$[Cp_2\mathbf{Ti}CC\mathbf{H}]_2$	6.48	6.54	20.26
4a	$[Cp_2\mathbf{Ti}CC\mathbf{SiH_3}]_2$	6.91	6.68	20.27
5a	$[Cp_2\mathbf{Zr}CC\mathbf{F}]_2$	6.05	6.33	38.08
6a	$[Cp_2\mathbf{Zr}CC\mathbf{CH_3}]_2$	6.61	6.40	38.11
7a	$[Cp_2\mathbf{Zr}CC\mathbf{H}]_2$	6.63	6.46	38.11
8a	$[Cp_2\mathbf{Zr}CC\mathbf{SiH_3}]_2$	7.01	6.64	38.11

These high values are explained considering that the decay of the electron density from the BCP in the direction perpendicular to the molecular plane is much more pronounced than in the direction contained in the plane, because in the latter direction the presence of metal atoms smoothes out the curvature of ρ(r), which becomes very reduced. These high ellipticity values have been associated by Bader[50] with a bond that is close to a formation or destruction process (also called catastrophe points). The proximity to this situation is reflected in the short distances between the BCP and the RCPs next to it, although the difference between them is measurable and well differentiated. The molecule nearest to that situation of bond creation/destruction is precisely **5a**, the molecule where ρ(r) and its Laplacian are the weakest, and the ellipticity is the highest. The fact that F promoted the existence of a $C_2-C_{2'}$ for a metal that usually does not allow this remote C−C interaction resulted in a very labile $C_2-C_{2'}$ bond.

Table 2 summarizes the electron populations integrated over the M, C_1, and C_2 QTAIM atomic basins. This table reveals two clear trends. The first one is the increasing charge as C_1 passes from Ti to Zr compounds. This increase is comparatively small (about 0.1 e$^-$) and is related to the different strength of the M−C bonds. The second trend correlates both C_1 and C_2 atomic charges with the substituents (R = F, CH_3, H, and SiH_3) electron-withdrawing character. Remarkably, the charge pull originated by R diminishes not only at its bonded atom (C_1) but also at C_2. This indicates that the charge has been transferred mainly from C_1-C_2 bonds, also supporting the above-described idea of partial bond destructions caused by highly electron-

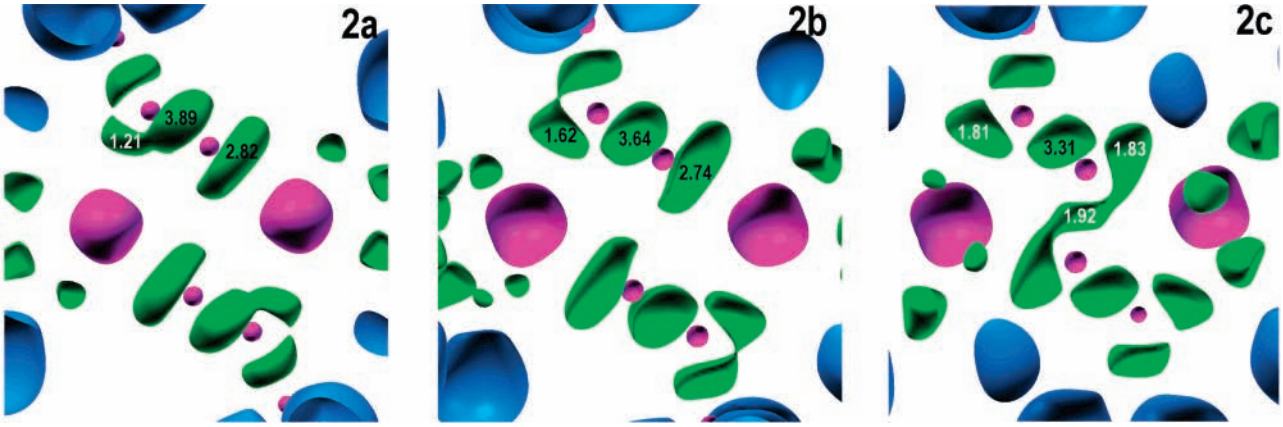

Figure 5. ELF isosurfaces of compound **2a**−**c** computed at a 0.75 ELF value. Numbers indicate the electron population of each basin. The color convention represents core basins in magenta, and the remaining valence basins are classified depending on the number of connections to core nuclear basins (synaptic order): red for monosynaptic, green for disynaptic, and cyan for disynaptic hydrogenated basins. Cp ligands have been omitted for clarity.

withdrawing substituents such as fluorine. By contrast, the metal atom charge remains almost unaltered by the different substituent, R.

An ELF analysis provides additional insight into the main effects that occur over the course of the reaction. Figure 5 displays the ELF basin evolution from **2a** to **2c**. Here, for **2a**, the formerly triple (in the monomer) C−C bond adopts a configuration very similar to a double bond, a basin population of 3.89 e^- with an elongated shape perpendicular to the molecular plane.[51] This is the result of attaching a Ti atom next to a triple C≡C bond, the partial destruction of its triple bond character. This diminution in bond order increases following the reaction from **2a** to **2c** and is noticed in a reduction of the C_1-C_2 basin population. This has remarkable consequences in the electron arrangement around the atoms composing the former triple bond (C_1 and C_2). The C_1 begins to acquire a basin arrangement similar to that of ethylene (two basins contained in the molecular plane in a fashion very similar to that of sp^2 hybridization) resulting in the displacement of the R substituent and causing the reduction of the $\angle RC_1C_2$ angle.

This effect, which is clear around the C_1 atomic position, is less evident for C_2. The C2−M basin presents minor changes upon evolution from **2a** to **2b**: In all cases, the basin is elongated and contained in the molecular plane, so this could be interpreted as a double bond between the C_2 and the M atoms, but the vicinity of $C_{2'}$ atom may change this. A detailed view of the basin's shape reveals that the elongation is different in the areas next to C_2, adopting a more acute shape. As the reaction reaches the transition state **2b**, this is more pronounced, and an approach between equivalent basins is observed.

The particular effects in the C_2-M basin resulting from the dimerization of two $RCCMCp_2$ can be better viewed when comparing the C−M valence basins with other organometallic compounds such as methyl metals.[52] For methyl metals, the M−C bonds present a high degree of ionic character. There is an electron transfer of about 1 e^- from the metal to the methyl group, located in the M−C basin. This basin presents a population near 2 e^- and is placed much nearer to C than to M, and it adopts a relatively small size with a C_3 symmetrical shape. When the situation of methyl metals is compared with the complexes studied here, the C−M basin of **1a**−**8a** shows a higher population (near 3 e^-), also a higher volume, and a prominently elongated shape along the molecular plane (and therefore, perpendicular to the C_1-C_2 basin); see Table-S8 in Supporting Information. The increase of population, volume, and anisotropy are precisely the same effects that take place around C_1. The ELF basin has gained about 0.8 e^- from the C_1-C_2 valence basin, and its shape spreads as a step prior to the formation of two basins, the same as already happened for C_1. It is noteworthy that the population reduction of the C_1-C_2 basin (about 2 e^-) is the sum of the C_1-M' (1.2 e^-) basin and the increase of the C_2-M basin (0.8 e^-). Given the position of the elongated basin, it is clear that a new bond is being formed, and because of the proximity of the basins, the $C_2-C_{2'}$ is promoted. Nevertheless, although QTAIM indicates the presence of a bond, no ELF basin corresponding to a $C_2-C_{2'}$ bond was found in the reactive complexes.

From the geometric, energetic, and electronic analyses discussed above, it could be deduced that the interaction that takes place between the two monomers is driven by the two different types of M−C interactions: the $M-C_2$ and $M-C_{1'}$. These two differ mainly in their geometrical arrangement: the first may be labeled as "frontal", because in reactive compounds, M, C_2, and C_1 are almost aligned, and the second may be identified as "lateral", because M gets closer to the opposite monomer sideways.

While the lateral bond results in the deterioration of the triple bond, the frontal bond allows an increase of population in the C_2-M basin resulting from the triple bond destruction. This is because the C_2-M ionic bond remains unchanged, regardless of the electrons pumped out from the former triple bond. If that bond was covalent, this electron flow would have not been favored, resulting in a destabilization of the system and, consequently, reducing the degree of destruction of the triple bond by the metal.

On comparing the behavior of the two M−C bonds, we find that, although the two bonds are relatively weak with an ionic character, one depends on the particular metal atom which it is bonded to, while the other does not. The bonding characteristics of $M-C_1$ remain almost identical (the same very low BCP values and same ELF population of about 1.2 e^-) for the equivalent Ti and Zr compounds. On the other hand, ELF population in $Zr-C_2$ bonds is systematically 10% higher than for $Ti-C_2$ bonds, but the respective density at their BCPs is 10% lower. This indicates that Zr frontal interactions are appreciably weaker than the Ti-equivalents, although the triple bond destruction induced by the Zr-lateral interaction is stronger than for Ti, a fact that again points out the differences in nature of these two bonding interactions.

The discussion of the nature of the long $C_2-C_{2'}$ bond raises questions about the main causes originating this unusually long C−C bond. Possible answers lie on the different metal radius, the electron-withdrawing character of R, and the surrounding of a transition metal atom. The overall picture of this work is varied, because from all the compounds studied, the C−C bond was found with both metals (Ti and Zr) and various C−C distances and substituents. However, the common point in all of these is the destruction of the triple C≡C bond, regardless of whether the long central C−C bond is formed or not.

It is evident that the condition necessary for the appearance of such a long C−C bond is the weakening of the triple bond, but there are also other factors that contribute and favor the presence of this bond. One of them is purely geometrical, the minimum distance to which both C_2 atoms are allowed to approach. In 1988, Jemmis[17] had already suggested the different metal size as a possible explanation of the different reactivity for Ti and Zr compounds.

Therefore, the possibility of forming a C_2-C_2 bond is greater for Ti, because its smaller atom size limits the approach between both C_2 atoms (about 2.7 Å). The corresponding distance for Zr-based compounds is higher, thus hampering the bond formation, but this is not an impediment: ELF study reveals that for Zr compounds the triple C≡C bond is also weakened in a fashion similar to that for Ti, but the two highly populated C_2-M basins (available to react with any radical) are too far apart to interact appropriately to form a bond. Therefore, other factors, such as the electron-withdrawing substituents (fluorine), are required to make the long C−C bond possible. These substituents pull charge from the triple bond, augmenting the destruction already started by the transition metal presence. This is readily visible in the reduction of the C_1-C_2 ELF valence basin as the electron-withdrawing character of R increases, an effect accompanied by an elongation of its shape, also translating as an increased ellipticity, reaching values close to those of standard double bonds.

As a result of the partial destruction of the C≡C triple bond, the distribution of the electron density around C_2 positions changes and the amount of charge between C_2 and M increases and distributes in order to form two pairing basins in the molecular plane, forming an angle with the C_2 center of about 120°, in an sp^2-like arrangement, and therefore increasing the possibility of forming a bond between C_2 and $C_{2'}$, increasing the minimum distance required to form this long bond.

Conclusions

The presence of an unexpected C−C bond of extraordinary length has been characterized for the first time in organometallic compounds with relevance to organic synthesis. This bond, which shows apolar characteristics and a length of about 2.7 Å for Ti complexes and 3.0 Å for Zr complexes, is found to be strongly correlated to the different thermodynamic character. The reactions in which this bond has been found (in the initial complexes) are favored in an average of 20 kcal·mol^{-1}, enough to change the reactions from endothermic to exothermic.

The presence of this bond is noticed not only in the relative stability of the products but also in the distribution of the electron density, where the QTAIM theory finds a bond path linking both C_2 atoms. The bond path crosses the area in between the two metal centers, a characteristic that stresses the relative strength, because the BCP has to constitute a maximum within the line that contains both metals, which is difficult due to the near presence of metal atoms.

The main cause of this bond is found in the partial destruction of the alkylidyne triple bond, caused by the presence of the Ti and Zr atoms, which reduce its bond order from triple to double. This destruction results in the development of new "lateral" bonding interactions between the C_1 and the metal atoms, while, simultaneously, the QTAIM and ELF characteristics indicate an increase in the accumulated charge of the "frontal" $M-C_2$ bond, in comparison to isolated metal alkylidynes. These modifications may take place only if the C_2-M bond is "flexible" enough to hold such accumulation of charge (increased in about 1 e$^-$) originated from the triple bond. This excess of charge close to C_2 and oriented toward $C_{2'}$ allows the formation of the incipient $C_2-C_{2'}$ bond, driving the subsequent reaction toward the final products. It is demonstrated that having a preformed bond in the reactives yields reactions more energetically favored.

Once the triple bond character has been diminished, an appropriate C···C distance is also required to lead to the formation of a bond path. In most circumstances, this bond is possible with distances of 2.7 Å, but not for 3.0 Å, which results in Zr-based reactive compounds not presenting the $C_2-C_{2'}$ bond. Nevertheless, the required values for the $C_2\cdots C_{2'}$ distance may change if highly electronegative substituents are attached to the alkylidyne unit.

So, as pulling charge from the triple bond favors its destruction, the presence of electronegative substituents results in an increase in the amount of charge accumulated next to C_2 and therefore in an increase of the bond-formation probability, reducing at the same time the minimum distance required. Fluorine is one of these substituents that is capable of inducing the presence of a $C_2-C_{2'}$ bond for Zr reactives (**5a**), where the $C_2-C_{2'}$ distance is up to 3.0 Å. The effect of F atom is so strong that, for Ti compound **1**, the products are so stabilized that the potential energy surface presents no barrier and thus no reactive or TS structure (**1a** and **1b**).

Therefore, the conditions needed and the factors that augment the transition metal activity for destroying and favoring the formation of this kind of long C−C bonds have been discovered, thus opening the possibility of improving the design of organometallic compounds for their use in oxidative coupling reactions.

Acknowledgment. This work has been financed by the "Consejería de Innovación Ciencia y Empresa-Junta de Andalucía" (ref FQM-840). We thank the "Centro y Servicios de Informática y Redes de Comunicaciones" (CSIRC), Universidad de Granada, for providing the computing time. We are grateful to Professor B. Silvi for supplying us a copy of the ToPMoD software package. Mr. David Nesbitt revised the English manuscript.

Supporting Information Available: Comparison between experimental and calculated bond distances of compounds **2a**−**8a** (Table S-1). Comparison between nonrelativistic and relativistic calculated bond distances of compounds **5a**−**8a** (Table S-2). Comparison between nonrelativistic and relativistic calculated activation energy of compounds **5a**−**8a** (Table S-3). Comparison between calculated bond distances of compounds **2b**−**8b** (Table S-4). Comparison between calculated bond distances of compounds **1c**−**8c** (Table S-5). Selected BCP parameters for **1b**−**8b** (Table S-6). Selected BCP parameters for **1c**−**8c** (Table S-7). ELF basin population of **2a**−**8a** (Table S-8). ELF basin population of **2b**−**8b** (Table S-9), ELF basin population of **1c**−**8c** (Table S-10). Integrated electron population over selected QTAIM atomic basins of **2b**−**8b** (Table S-11). Integrated electron population over selected QTAIM atomic basins of **1c**−**8c** (Table S-12). Laplacian of electron density

plot of **1**(**a**−**c**)−**8**(**a**−**c**) compounds (Figure S-13). Graphical representation of the bond path's, ring critical points and bond critical point of compound **4a** (Figure S-14). Optimized molecular structures of **1**(**a**−**c**)−**8**(**a**−**c**) (Table S-15). This material is available free of charge via the Internet at http://pubs.acs.org.

References and Notes

(1) Oliva, J. M.; Allan, N. L.; Schleyer, P. v. R.; Vinas C.; Teixidor F. *J. Am. Chem. Soc.* **2005**, *127*, 13538.

(2) Toda, F.; Tanaka, K.; Watanabe, M.; Tamura, K.; Miyahara, I.; Nakai, T.; Hirotsu, K. *J. Org. Chem.* **1999**, *64*, 3102.

(3) Novoa, J. J.; Lafuente, P.; Del Sesto, R. E.; Miller, J. S. *Angew. Chem., Int. Ed.* **2001**, *40*, 2540.

(4) Hirano, M.; Shibasaki, T.; Komiya, S.; Bennett, M. A. *Organometallics* **2002**, *21*, 5738.

(5) Fellmann, J. D.; Schrock, R. R.; Traficante, D. D. *Organometallics* **1982**, *1*, 481.

(6) Grubbs, R. H.; Coates, G. W. *Acc. Chem. Res.* **1996**, *29*, 85.

(7) Bader, R. F. W.; Matta, C. F. *Organometallics* **2002**, *23*, 6253.

(8) Vidal, I.; Melchor, S.; Alkorta, I.; Elguero, J.; Sundberg, M. R.; Dobado, J. A. *Organometallics* **2006**, *25*, 5638.

(9) Clot, E.; Eisenstein, O. *Struct. Bonding* **2004**, *113*, 1.

(10) Scherer, W.; McGrady, G. S. *Angew. Chem., Int. Ed.* **2004**, *43*, 1782.

(11) Sekutowski, D. G.; Stucky, G. D. *J. Am. Chem. Soc.* **1976**, *98*, 1376.

(12) Teuben, J. H.; de Liefde Meijer, H. J. *J. Organomet. Chem.* **1969**, *17*, 87.

(13) Crabtree, R. H. *The Organometallic Chemistry of Transition Metal*; John Wiley: New York, 1994.

(14) Erker, G.; Frömberg, W.; Reinhard, B.; Richard, M.; Angermund, K.; Krüger, C. *Organometallics* **1989**, *8*, 911.

(15) Cuenca, T.; Gómez, R. M.; Gómez-Sal, P.; Rodríguez, G. M.; Royo, P. *Organometallics* **1992**, *11*, 1229.

(16) Scoles, L.; Minhas, R.; Duchateau, R.; Jubb, J.; Gambarotta, S. *Organometallics* **1994**, *13*, 4978.

(17) Kumar, P. N. V. P.; Jemmis, E. D. *J. Am. Chem. Soc.* **1988**, *110*, 125.

(18) (a) Rosenthal, U. M.; Pellny, P. M.; Kirchbauer, F. G.; Burlakov, V. V. *Acc. Chem. Res.* **2000**, *33*, 119. (b) Baumann, W.; Pellny, P. M.; Rosenthal U. *Magn. Reson. Chem.* **2000**, *38*, 515. (c) Pellny, P. M.; Peulecke, N.; Burlakov, V. V.; Baumann, W.; Spannenberg, A.; Rosenthal, U. *Organometallics*, **1999**, *19*, 1198. (d) Rosenthal, U. *Angw. Chem., Int. Ed.* **2003**, *42*, 1794. (e) Rosenthal, U.; Arndt, P.; Baumann, W.; Burlakov, V. V.; Spannenberg, A. *J. Organomet. Chem.* **2003**, *670*, 84. (f) Rosenthal, U.; Arndt, P.; Baumann, W.; Burlakov, V. V.; Spannenberg, A. *Organometallics* **1999**, *24*, 456. (g) Burlakov, V. V.; Arndt, P.; Baumann, W.; Spannenberg, A.; Rosenthal, U.; Parameswaran, P.; Jemmis, E. D. *Chem. Commun.* **2004**, 2074.

(19) Dobado, J. A.; Martínez-García, H.; Molina, J.; Sundberg, M. R. *J. Am. Chem. Soc.* **2000**, *122*, 1144.

(20) Dobado, J. A.; Molina, J.; Uggla, R.; Sundberg, M. R. *Inorg. Chem.* **2000**, *39*, 2831.

(21) Choukroun, R.; Donnadieu, B.; Zhao, J.; Cassoux, P.; Lepetit, C.; Silvi, B. *Organometallics* **2000**, *19*, 1901.

(22) Frisch, M. J.; Trucks, G. W.; Schlegel, H. B.; Scuseria, G. E.; Robb, M. A.; Cheeseman, J. R.; Montgomery, J. A., Jr.; Vreven, T.; Kudin, K. N.; Burant, J. C.; Millam, J. M.; Iyengar, S. S.; Tomasi, J.; Barone, V.; Mennucci, B.; Cossi, M.; Scalmani, G.; Rega, N.; Petersson, G. A.; Nakatsuji, H.; Hada, M.; Ehara, M.; Toyota, K.; Fukuda, R.; Hasegawa, J.; Ishida, M.; Nakajima, T.; Honda, Y.; Kitao, O.; Nakai, H.; Klene, M.; Li, X.; Knox, J. E.; Hratchian, H. P.; Cross, J. B.; Bakken, V.; Adamo, C.; Jaramillo, J.; Gomperts, R.; Stratmann, R. E.; Yazyev, O.; Austin, A. J.; Cammi, R.; Pomelli, C.; Ochterski, J. W.; Ayala, P. Y.; Morokuma, K.; Voth, G. A.; Salvador, P.; Dannenberg, J. J.; Zakrzewski, V. G.; Dapprich, S.; Daniels, A. D.; Strain, M. C.; Farkas, O.; Malick, D. K.; Rabuck, A. D.; Raghavachari, K.; Foresman, J. B.; Ortiz, J. V.; Cui, Q.; Baboul, A. G.; Clifford, S.; Cioslowski, J.; Stefanov, B. B.; Liu, G.; Liashenko, A.; Piskorz, P.; Komaromi, I.; Martin, R. L.; Fox, D. J.; Keith, T.; Al-Laham, M. A.; Peng, C. Y.; Nanayakkara, A.; Challacombe, M.; Gill, P. M. W.; Johnson, B.; Chen, W.; Wong, M. W.; Gonzalez, C.; Pople, J. A. Gaussian 03, revision B.05; Gaussian, Inc.: Wallingford, CT, 2004.

(23) Becke, A. D. *J. Chem. Phys.* **1993**, *98*, 5648.

(24) Lee, C.; Yang, W.; Parr, R. G. *Phys. Rev. B* **1988**, *37*, 785.

(25) Møller, C.; Plesset, M. S. *Phys. Rev.* **1934**, *46*, 618.

(26) Godbout, N.; Salahub, D. R.; Andzelm, J.; Wimmer, E. *Can. J. Chem.* **1992**, *70*, 560.

(27) Sosa, C.; Andzelm, J.; Elkin, B. C.; Wimmer, E.; Dobbs, K. D.; Dixon, D. A. *J. Phys. Chem.* **1992**, *96*, 6630.

(28) Stevens, W. J.; Krauss, M.; Basch, H.; Jasien, P. G. *Can. J. Chem.* **1992**, *70*, 612.

(29) Seeger, R.; Pople, J. A. *J. Chem. Phys.* **1977**, *66*.

(30) Bauernschmitt, R.; Ahlrichs, R. *J. Chem. Phys.* **1996**, *104*, 9047.

(31) Bader, R. F. W. *Atoms in Molecules: A Quantum Theory*; Clarendon Press: Oxford, U.K., 1990.

(32) Bader, R. F. W. *Chem. Rev.* **1991**, *91*, 893.

(33) Bader, In *Encyclopedia of Computational Chemistry*; Schleyer, P. v. R., Ed.; Wiley: Chichester, U.K., 1998.

(34) Becke, A. D.; Edgecombe, K. E. *J. Chem. Phys.* **1990**, *92*, 5397.

(35) Silvi, B.; Savin, *Nature* **1994**, *371*, 683.

(36) Sivi, B.; Fourré, I.; and Alikhani, M. E. *Monatsh. Chem.* **2005**, *136*, 855.

(37) Silvi, B. *Phys. Chem. Chem. Phys.* **2004**, *6*, 256.

(38) Noury, S.; Krokidis, X.; Fuster, F. and Silvi, B. *Comput. Chem.* **1999**, *23*, 597.

(39) MORPHY98, a program written by P. L. A. Popelier with a contribution from R. G. A. Bone; UMIST, Manchester, U.K., 1998.

(40) Popelier, P. L. A. *Comput. Phys. Commun.* **1996**, *93*, 212.

(41) Popelier, P. L. A. *Chem. Phys. Lett.* **1994**, *228*, 160.

(42) Biegler-König, F.; Schönbohm, J.; Bayles, D. *J. Comput. Chem.* **2001**, *22*, 545.

(43) Pepcke, E.; Lyons, J. SciAn 1.2; SCRI, Florida State University, Tallahassee, FL, 1996.

(44) Metzler, N.; Noeth, H. *J. Organomet. Chem.* **1993**, *454*, C5.

(45) Wood. G. L.; Knobler, C. B.; Hwathorne, M. F. *Inorg. Chem.* **1989**, *28*, 282.

(46) Allen, F. H. *Acta Crystallogr., Sect. B: Struct. Crystallogr. Cryst. Chem.* **2002**, *58*, 380.

(47) Jemmis, E. D.; Giju, K. T. *J. Am. Chem. Soc.* **1998**, *120*, 6952.

(48) Dobado, J. A.; Molina, J. M. *J. Phys. Chem.* **1994**, *98*, 1819.

(49) The value of the hypothetical reaction from **1a** to **1c** was calculated as the difference between the stable product structure **1c** and that of a nonequilibrium geometry with a $C_2-C_{2'}$ bond distance similar to that of the most reactive structures (2.9 Å).

(50) Wiberg, K. B.; Bader, R. F. W.; Lau, C. D. H. *J. Am. Chem. Soc.* **1987**, *109*, 985.

(51) This basin presents two different attractors, one above and other below the molecular plane. The value of the basin population displayed is the result of adding the corresponding charges for both attractors.

(52) Vidal, I.; Melchor, S.; Dobado, J. A. *J. Phys. Chem. A* **2005**, *109*, 7500.